Hindawi
Mathematical Problems in Engineering
Volume 2024, Article ID 7021298, 15 pages
https://doi.org/10.1155/2024/7021298

Research Article

Analysis and Simulation of Lateral Collision Risk under Paired Approach

Fei Lu, Jian Zhang, Haonan Chen, and Zichen Chen

College of Air Traffic Management, Civil Aviation University of China, Tianjin 300300, China

Correspondence should be addressed to Fei Lu; lufei315@126.com

Received 21 June 2023; Revised 31 January 2024; Accepted 5 February 2024; Published 29 March 2024

Academic Editor: Yi Xue

The paired approach can improve the efficiency of closely spaced parallel runways. Calculating the probability and frequency of horizontal overlap is an indispensable step when evaluating the horizontal collision risk of the paired approach. As the generation of horizontal overlap probability is closely related to horizontal position error, we propose a calculation method of horizontal overlap probability based on position error from the perspective of pilot operation. First, according to the principle of flight mechanics, the attitude adjustment model is established for the horizontal direction of the approach process, and the pilot's operation model for various position errors is based on the concept of the stochastic process. This attitude adjustment model can replicates the process of the pilot operating the steering column to change the aircraft's attitude. When combined with the pilot's operation model, it is possible to simulate the position errors generated during the approach process. Building on this, the horizontal overlapping conditions of two aircraft are analyzed to simulate the horizontal overlap process in the paired approach. The duration and instances of overlap counted and the ratio between these results and the total running time give the overlap probability and frequency. Multiple simulations in MATLAB reveal that higher pilot operating accuracy shortens the time for the aircraft to align with the course, whereas lower accuracy leads to unstable horizontal position errors. Furthermore, the horizontal overlap in paired approaches primarily occurs at the beginning of the procedure, and enhancing the pilot's operating accuracy does not significantly affect the probability and frequency of horizontal overlap.

1. Introduction

With the increasing number of take-off and landing flights at airports in China, the incidence of flight delays caused by long waiting times is also on the rise. The primary cause of this issue is the saturation of airport runway capacity. While building new runways or airports is the usual solution, the limitation of land resources often makes it feasible only to construct closely spaced parallel runways. Two parallel runways with a distance of less than 760 m are defined as closely parallel runways. Due to wake turbulence, aircraft taking off or landing on closely parallel runways must maintain the same radar interval as on common runways, which means the runway capacity is not significantly improved. To address this, NASA proposed the paired approach procedure for closely spaced parallel runways [1], which demands higher standards for navigation and monitoring equipment on the two paired aircraft.

The paired approach requires the trailing aircraft to stay ahead of the wake turbulence of the leading aircraft to avoid it. Therefore, if two aircraft come into contact or the trailing aircraft enters the wake of the leading aircraft, it is considered a collision. When implementing the paired approach procedure, the longitudinal spacing between the two aircraft must meet the following requirements:

(1) Avoid airframe contact: The trailing aircraft must maintain a safe distance from the leading aircraft to prevent collision.
(2) Avoid wake contact: The trailing aircraft must remain close enough to the leading aircraft to avoid its wake turbulence.

The paired approach can effectively enhance the capacity of closely parallel runways. However, its safety has been a

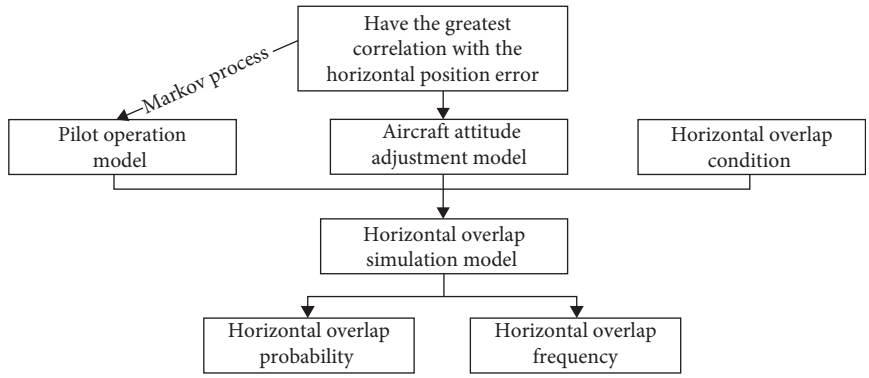

Figure 1: Research process.

subject of ongoing debate since its introduction due to its unique operational mode.

Research in this field has been carried out since 2000. The research results of Torres-Pomales et al. [2] showed that assigning different glide paths to aircraft pairs could improve the safety of paired approach operations. Geyer et al. [3] established an error system model based on the Regional Navigation and Global Positioning System when studying the wake collision risk of paired approaches. Landry and Prichett [4] put forward the concept of the safety zone, modeled it, and studied the factors affecting the scope of the safety zone. Teo et al. [5] presented a real-time calculation method for dangerous areas, which could warn aircraft to take evasive maneuvers in case of a false approach. Madden [6] analyzed the influence of leading and trailing aircraft speeds on safety from the kinematic point of view and determined the longitudinal safety separation.

Fei et al. [7, 8] evaluated the lateral and longitudinal collision risks of the paired approach by analyzing the distribution of positioning errors and the operation process of the paired approach. Zongping et al. [9] established a collision model combining acceleration error and navigation error distribution and calculated the longitudinal collision risk of the paired approach. Runping et al. [10] established a kinematic model and compared and analyzed the impact of related parameters, such as initial interval, on collision risk. Zhaoning and Xiaoxu [11] analyzed the safety of the rear aircraft by establishing a take-off safety zone model and clarified the speed relationship between leading and trailing aircraft during paired take-off. Lili et al. [12] improved the calculation method for the safety zone by establishing a microscopic car-following model. Fei et al. [13, 14] established a torque balance equation on the premise that the aircraft could bear a certain induced rolling torque and established a collision model based on the error distribution to evaluate the safety separation between two aircraft. This concept increased the safety area of paired approaches. Fei et al. [15] put forward a simulation and calculation method for flight trajectory, as well as the collision risk calculation method and wake vortex encounter risk calculation method. Fei et al. [16] extracted the ocean tracks in space-based ADS-B data, a collision risk model based on the Bayesian network is established, and the error distribution parameters and occurrence frequency are brought into the model to evaluate the collision risk of parallel routes in the ocean area. Lu et al. [17] present a method to calculate vertical overlap probability based on the position error caused by pilot control.

In fact, the assessment of collision risk can be regarded as the premise for calculating the safety interval. Thus, an accurate calculation method is needed. Collision risk is usually calculated from three directions [18–20]. The basic parameters for the calculation are the overlapping probability and frequency of horizontal, longitudinal, and lateral directions. Overlapping in the horizontal direction means that there is a lateral collision between two aircraft, which is caused by the horizontal position error. Previous scholars often analyze the position error directly from the angle of error distribution without considering the influence of pilot operation.

In view of this, we present an aircraft attitude adjustment model for operating parameters that have the greatest correlation with the horizontal position error in the approach process. Based on regular statistics of the parameters, the idea of a stochastic process is employed to establish the pilot operation model. Finally, the horizontal overlap condition, considering the wake motion characteristics, is added to establish a horizontal overlap simulation model for a paired approach. Through the operation of the simulation model, the horizontal overlap time and the number of overlaps are counted, and then the overlap probability and frequency are calculated. The research process of this paper is illustrated in Figure 1.

2. Aircraft Attitude Adjustment Model

According to the results of the analysis by Zhaoning et al. [21], the quick access recorder (QAR) parameters related to pilot operation are the positions of the steering wheel and rudder. QAR data is a kind of flight data recorder, which can record hundreds of parameters from takeoff to landing, including aircraft performance, pilot operation, cockpit input, and so on. The lateral position error in this paper is the course deviation in QAR parameters, which refers to the deviation of the aircraft track from the center line of the course.

In order to determine the influence of the steering wheel and rudder on the horizontal position error, it is necessary to start with the mapping relationship between them and the horizontal attitude of the aircraft. In the approach process, the position of the steering wheel is the most frequent among

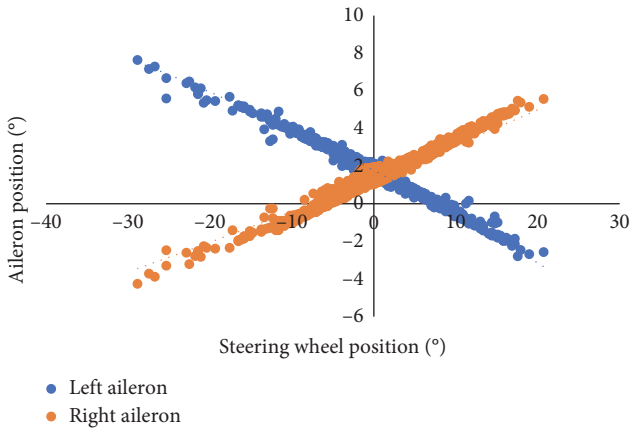

Figure 2: Direct correspondence rule.

the QAR parameters. Therefore, when studying the probability of horizontal overlap, we focus on the steering wheel factor as a change in the plane's horizontal attitude will cause a corresponding course deviation, which in turn will affect the calculation of collision risk.

2.1. Direct Correspondence Rule. The horizontal control of the aircraft includes directional control and lateral control. A pilot completes directional control using the pedal and completes the lateral control by turning the steering wheel left and right. The corresponding relationship between the pedal and the rudder is denoted as $\delta_{\text{Direct}} = f_{\text{Direct}}(d)$. When the airplane is stationary, one pedal angle corresponds to one rudder position. This corresponding relationship is called the "direction direct correspondence" rule, while the relationship between the airplane's steering wheel and aileron follows a "lateral direct correspondence" rule $\delta_{\text{aileron}} = f_{\text{steer}}(d)$.

We take the "horizontal direct correspondence" rule as an example, as shown in Figure 2.

As shown in Figure 2, when the steering wheel position is 0°, the deflection angle of the left and right ailerons is 2° because the ailerons on both sides of the plane serve as flaps and provide more lift. At the same time, we can see that the direct correspondence between the rule of left and right ailerons is symmetrical, occurring at about $y = 2$, which means that the deflection amplitude of both ailerons is the same when the steering wheel position is changed.

2.2. Horizontal Moment and Aircraft Attitude. The lateral attitude of the aircraft is controlled by both directional control and lateral control [22].

In this paper, the dimensionless moment coefficient m, which is commonly used in engineering and research, is utilized to analyze the stress problem of aircraft [23].

$$m = \frac{M}{\frac{1}{2}\rho V^2 S l} \Rightarrow M = \frac{m}{\frac{1}{2}\rho V^2 S l}. \tag{1}$$

Here, M is the moment on the aircraft, m is the moment coefficient, ρ is the atmospheric density, v is the relative inflow velocity, s is the analyzed airfoil or rudder surface, and l is the arm length.

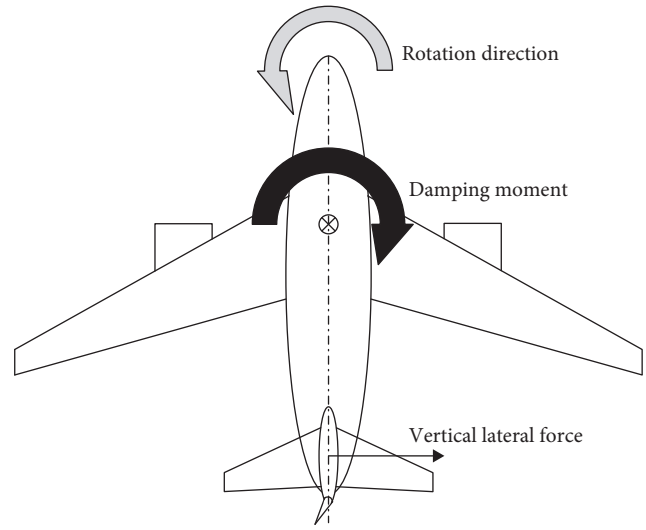

Figure 3: Direction damping moment.

2.2.1. Direction Control. When the pilot conducts directional control, the aircraft will be subjected to the combined action of the directional control moment M_{xd}, the directional stability moment M_{xv}, and the directional damping moment M_{xo}.

The directional control moment is mainly generated by operating the rudder pedal and changing the position of the rudder surface.

The main sources of the directional stability moment are the fuselage and the vertical tail, where the directional stability moment generated by the fuselage is far less than that of the vertical tail. Therefore, we mainly consider the vertical tail in the modeling.

When there is a yaw moment on the aircraft, it will rotate around the vertical axis, leading to an additional lateral airflow velocity component at the vertical tail, which will generate lateral force (as shown in Figure 3). When the nose of the airplane turns left, the vertical tail moves to the right, and both the additional airflow and the lateral force on the vertical tail are in the left direction. The lateral force helps prevent the nose of the aircraft from continuing to lean to the left, which is called the directional damping moment. While other components can also generate a directional damping moment, this moment generated by the vertical tail accounts for 97.9% of the whole aircraft, which means the other components can be ignored.

The change of the resultant moment causes a change in the aircraft side slip angular velocity, and the relation formula is as follows:

$$\alpha_{xd} = \frac{M_d}{I_d}, \quad \omega_{xd} = \int \alpha_{xd} dt, \tag{2}$$

where α_{xd} is the sideslip angular acceleration, M_d is the directional resultant moment, and ω_{xd} is the sideslip angular velocity, and I_d is the directional moment of inertia.

While calculating the rotary inertia, the object of the model is only the vertical tail. In order to simplify the model, we regard the vertical tail as an equivalent cuboid, as shown in Figure 4, where the cylinder represents the fuselage.

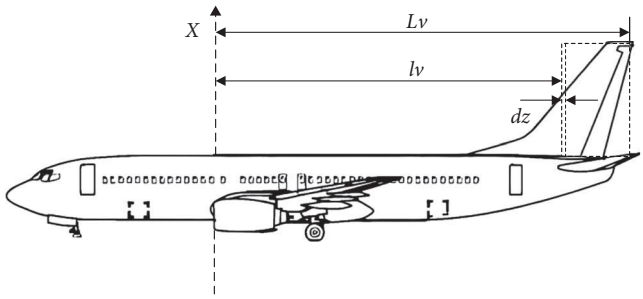

Figure 4: Direction moment of inertia model.

We establish the aircraft directional and attitude adjustment model for the vertical tail and rudder as follows [23]:

$$\begin{cases} M_{xv} = \dfrac{-a_v \beta k \rho V^2 S_v L_v}{2} \\ M_{xo} = -\dfrac{1}{2}\sqrt{k}\rho V a_v S_v L_v^2 \omega_{xd} \\ M_{xd} = \dfrac{-k a_v \eta_{xd} \rho V^2 S_v L_v \delta_v}{2} \\ M_d = M_{xv} + M_{xo} + M_{xd} \\ \delta_d = f_d(d) \\ I_d = \displaystyle\int_{l_v}^{L_v} z^2 dm_v = \int_{l_v}^{L_v} z^2 \frac{m_v}{L_v - l_v} dz, \end{cases} \tag{3}$$

where M_{xd} is the steering moment produced by the vertical tail, and the lateral force of the vertical tail generally acts behind the center of gravity. When the rudder is turned left, it can produce the deflection moment in the opposite direction, so $M_{x\psi}$ is negative. M_{xo} is the directional damping moment. Also, due to the change in the relative airflow speed and direction at the vertical tail, additional lateral force is formed, which forms a moment opposite to the rotation direction of the aircraft relative to the center of gravity, preventing the aircraft from deviating further from the original equilibrium position. $M_{x\psi}$ is the directional stability moment. When the direction of the relative airflow at the vertical tail changes, it generates aerodynamic force in the opposite direction to the relative airflow, forming a deflection moment at the center of gravity, so that the aircraft automatically tends to restore the original directional balance state.

a_v is the slope of the vertical tail side force coefficient curve; β is the side slip angle; k is the speed deceleration coefficient, $k<1$; S_v is the area of the vertical tail. Additionally, L_v is the distance from the vertical tail to the center of gravity of the aircraft; η_{xd} is the rudder efficiency; δ_d is the rudder deflection angle, where the left deflection is negative; $\delta_d = f_d(d)$ is the direct correspondence rule between the pedal and the rudder; m_v is the vertical tail mass.

2.2.2. Lateral Control. When pilots carry out lateral control, the center of gravity of the aircraft will be affected by the lateral control moment generated by the aileron deflection, the lateral stability moment, and the lateral damping moment.

The lateral control moment is mainly generated by the steering wheel operation and comes from the wing dihedral angle, wing sweep angle, and the vertical tail. The relationship between the rolling damping moment of the aircraft and the rolling direction is shown in Figure 5. The wing, horizontal tail, and vertical tail of the airplane can all generate the rolling damping moment. However, as the damping moment generated by the wing accounts for about 98.4% of all components, only the wing part is mainly considered in the model, and others are ignored.

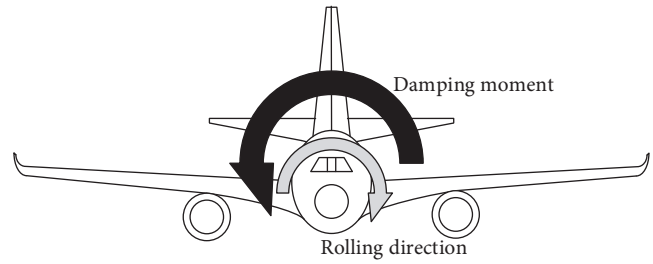

Figure 5: Lateral damping moment.

The change of lateral moment causes a change in the aircraft roll angular velocity. The relation formula is as follows:

$$\alpha_{xl} = \frac{M_l}{I_l},\ \omega_{xl} = \int \alpha_{xl} dt, \tag{4}$$

where α_{xl} is the roll angular acceleration, M_l is the lateral moment, I_l is the lateral moment of inertia, and ω_{xl} is the roll angular velocity.

While calculating the moment of inertia, the main object of the model is the wing. In order to simplify the model, we consider the wing as a cuboid (as shown in Figure 6), and the width of the cuboid is the mean aerodynamic chord of the wing. Additionally, the fuselage is regarded as a cylinder.

We establish the lateral attitude adjustment model of the aircraft's wing and aileron as follows [23]:

$$\begin{cases} M_{x\psi} = -a\beta\psi\rho V^2 \displaystyle\int_0^{l/2} xb\, dx \\ M_{x\chi} = -\beta C_y \rho V^2 \sin\chi \displaystyle\int_0^{l/2} xb\, dx \\ M_{\mathrm{xlo}} = \displaystyle\int M_{xl}^{\omega_{xl}} d\omega_{xl} = \frac{1}{4}\int m_x^{\overline{\omega}_{xl}} \rho V S_w l^2 d\omega_{xl} \\ M_{\mathrm{xlv}} = \dfrac{-a_v \beta k \rho V^2 S_v y_v}{2} \\ M_{xa} = \dfrac{-a_v \eta_{xa} \delta_a \rho V^2 S_x l_x}{4} \\ M_l = M_{x\psi} + M_{x\chi} + M_{\mathrm{xlo}} + M_{xv} + M_{xa} \\ \delta_a = f_s(d) \\ I_l = \dfrac{\displaystyle\int_{\frac{-l}{2}}^{\frac{l}{2}} x^2 \frac{m_w}{l} dx = m_w l^2}{12}, \end{cases} \tag{5}$$

where $M_{x\psi}$ is the stabilizing moment generated by the dihedral angle, when the aircraft is disturbed and has a slope, due to the effect of the dihedral angle, the angle of attack of the upwind wing increases and the lift increases, while the lift of the downwind wing

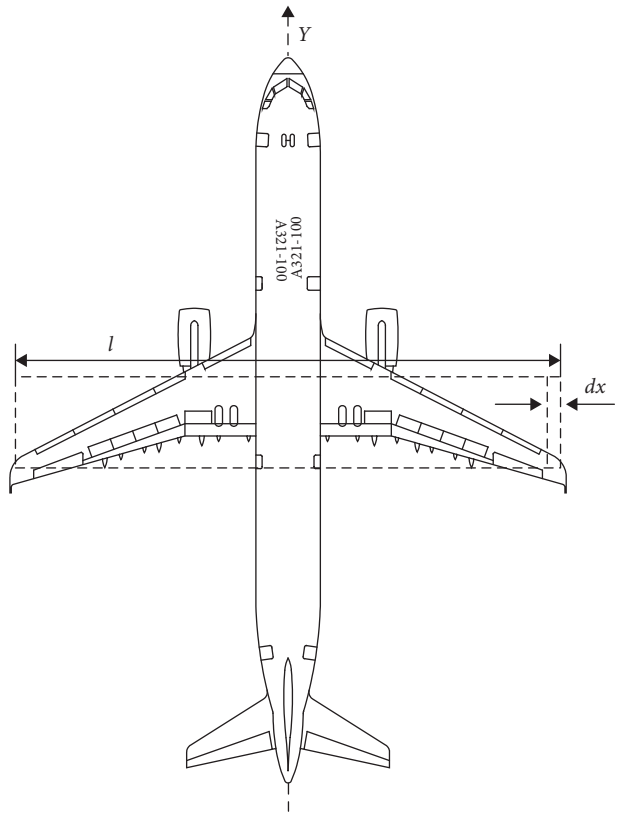

Figure 6: Lateral moment of the inertia model.

decreases. Thus, the difference between the lift of the wings on both sides forms a rolling moment, trying to eliminate the slope and make the aircraft have the tendency to automatically restore the original lateral balance. ψ is the dihedral angle, l is the wingspan of the aircraft, b is the section chord, $M_{x\chi}$ is the stabilizing moment generated by the angle of sweep back. In the left roll, the effective split speed of the left wing of the aircraft is greater than that of the right wing, so the difference in lift between the two wings forms the lateral stability moment. C_y is the lift coefficient of the aircraft, χ is the sweep back angle of the aircraft, M_{xlo} is the lateral damping moment, when the aircraft is disturbed and rolled, the local angles of two wings are not equal, and the angle of attack of the ascending wing will decrease, while the angle of attack of the descending wing will increase, resulting in the unequal lift of the wings on both sides, resulting in a rolling moment that hinders rotation. M_{xlv} is the lateral stabilizing moment generated by the vertical tail, and y_v is the distance from the center of gravity of the aircraft to the side force along the Y-axis direction. Additionally, $M_{xo}^{\omega_{xl}}$ is the derivative of the lateral damping moment relative to angular velocity, $m_x^{\overline{\omega}_{xl}}$ is the derivative of the lateral rolling moment coefficient relative to dimensionless value $\overline{\omega}_{xl}$, S_w is the wing area, M_{xaw} is the lateral control moment generated by aileron operation, η_{xa} is the aileron efficiency, δ_a is the aileron deflection angle, S_x is the total surface area of the aileron, l_x is the distance between the center positions of the left and right ailerons, M_l is the lateral resultant moment, $\delta_a = f_s(d)$ is the direct correspondence rule between the steering wheel and the aileron, and m_w is the mass of the wing.

In directional control, the rudder deflection angle corresponds to the side slip angle; in vertical control, the elevator deflection angle corresponds to the angle of attack. Unlike the previous two controls, when the pilot turns the steering wheel, an aileron deflection angle will correspond to a roll angular velocity, not a roll angle. Therefore, as it is difficult to obtain an accurate aircraft attitude by modeling ailerons, it is impossible to conduct follow-up research. According to the results of the analysis by Guerreiro and Neitzke [24], the roll angle is also related to course deviation, and the roll angle of the aircraft is also the embodiment of the pilot's lateral control. In order to make the research more accurate, we use the roll angle as the pilot lateral control parameter in this work.

3. Pilot Operation Model Based on the Markov Process

Figure 7 shows the QAR data of the heading course deviation recorded by seven aircraft entering the final approach stage at the same airport. It can be seen that there is an error when the aircraft enters the final approach stage, and the pilot will adjust the attitude of the aircraft to make the flight path coincide with the heading course. Pilots will usually operate accurately according to their experience. However, incorrect operations or deviations can occur.

As the pilot's operation is only related to the current aircraft state (course deviation), we consider this as a Markov process and establish a pilot operation model based on this

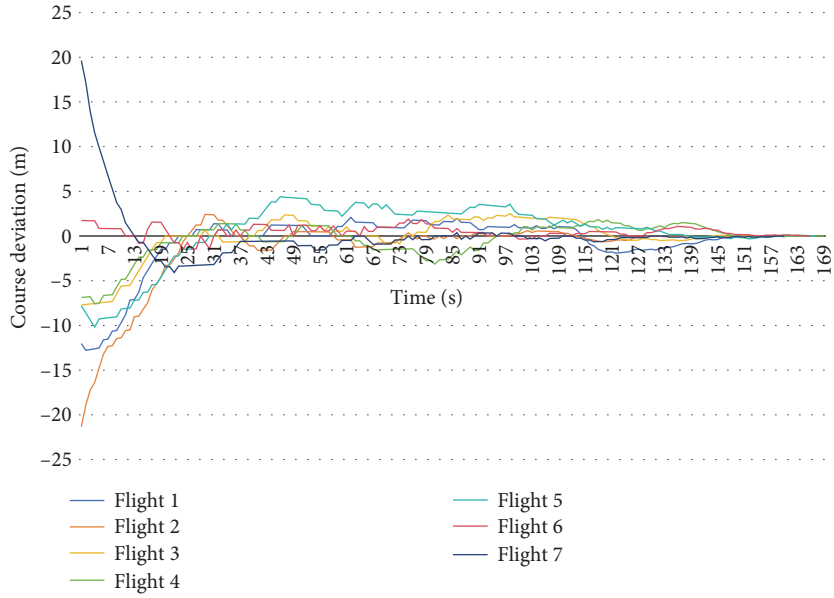

Figure 7: Course deviation after the aircraft cuts into the final approach stage.

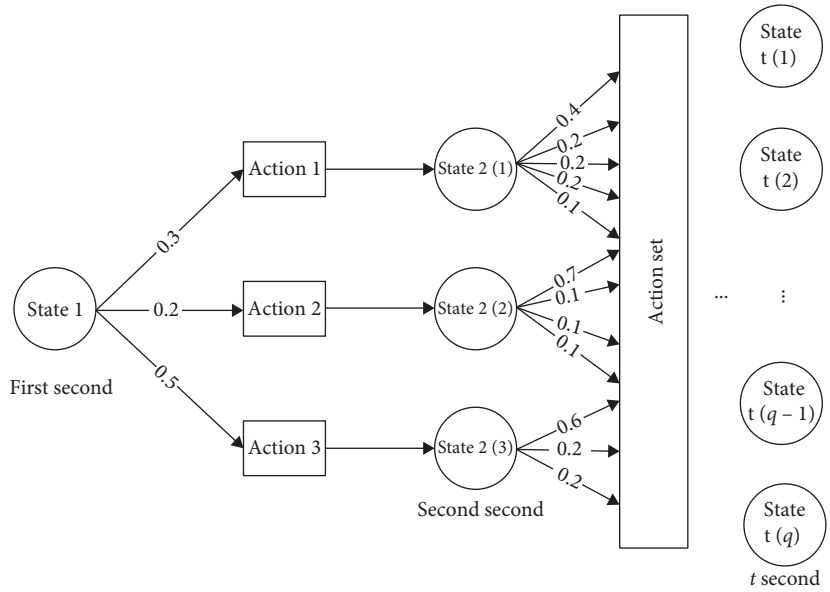

Figure 8: Stochastic process model of pilot operation.

concept. The flight state set is recorded as $S = \{s_1, s_2, \ldots, s_n\}$, the pilot action set is recorded as $D = \{d_1, d_2, \ldots, d_m\}$, and the probability of the pilot taking the operation action d_m when the aircraft is in the state s_n is $P_{nm} = P(d_m | s_n)$. The state-action matrix P is then defined as follows:

$$P = \begin{bmatrix} P_{11} & \cdots & P_{1m} \\ \vdots & \ddots & \vdots \\ P_{n1} & \cdots & P_{nm} \end{bmatrix}. \tag{6}$$

For any $i \in (1, n)$, $\sum_{k=1}^{m} P_{ik} = 1$.

If the state of t at the time of the paired approach is S_t, then the state at time $t+1$ will be $s_{t+1} = s_t + \Delta s$, and

$$\Delta s = \int (V + a_j) \sin \beta + V_l dt, \tag{7}$$

$$V_l = \int \frac{\rho V^2 C_y S_w \sin \gamma}{2m} dt, \tag{8}$$

where a_j is the longitudinal acceleration of the aircraft, V_l is the lateral speed, C_y is the lift coefficient of the aircraft, and m is the mass of the aircraft.

The pilot operation model and the total approach process are described in Figure 8.

Obviously, the probability of pilots taking actions varies under different states, and the matrix P will also change,

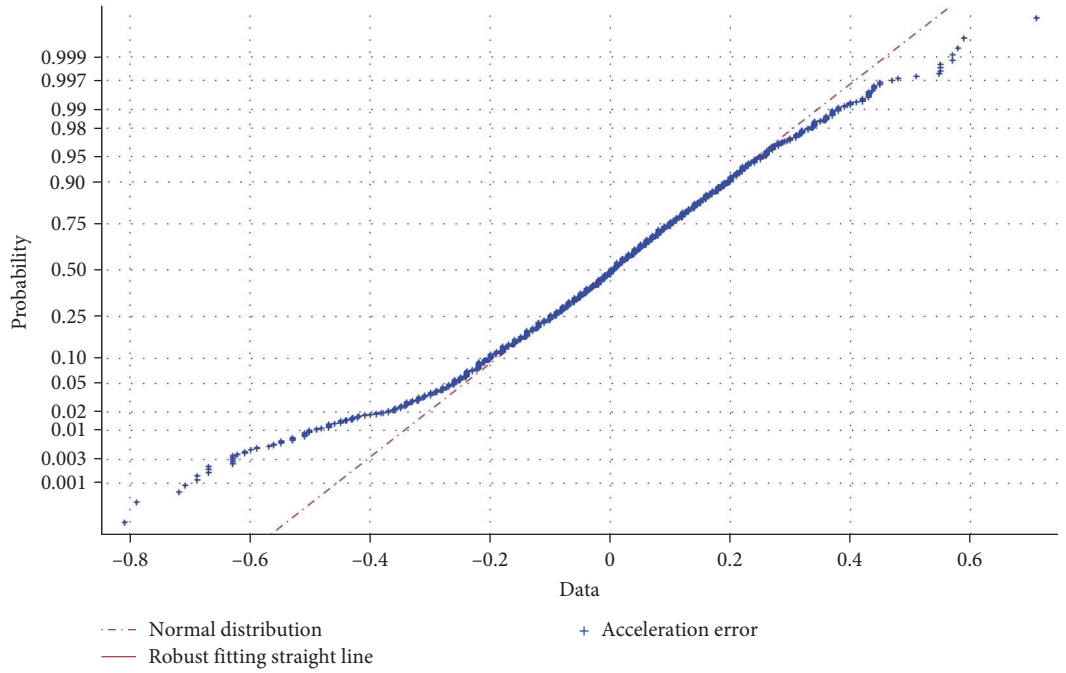

Figure 9: Normal distribution fitting.

Table 1: Output of normal distribution test.

Muhat	Sigmahat	Muci	Sigmaci
−0.00281	0.165198	(−0.0080498467366, 0.002421207943)	(0.16157818234, 0.16898441576)
h		Sig	
0		1	

affecting the whole approach process. Therefore, we introduce the correct rate of operation P_{Correct}, which is defined as the probability that pilots will take correct actions when an aircraft is in a certain state. Correct operation means that this action is beneficial for the aircraft to lock the course, while failure to do so will make the aircraft deviate from the course.

$$P_{\text{Correct}} = \frac{C_{\text{Correct}}}{C_A}, \tag{9}$$

where C_{Correct} is the number of times that the pilot takes correct actions, and C_A is the total number of the pilot's actions. The criteria for judging a correct action are as follows:

$$\begin{cases} a > 0, s < 0 \\ a = 0, s = 0 \\ a < 0, s > 0 \end{cases}. \tag{10}$$

4. Paired Approach Horizontal Overlap Simulation Model

The longitudinal acceleration error of the aircraft must be considered when establishing the horizontal overlap model.

As there is no strict requirement for acceleration during an approach, and there is no standard comparable to that of heading course and glide slope. Therefore, when we calculate the acceleration error, we take the average longitudinal acceleration of 30 flights in their final approach stage as the nominal acceleration.

The output is shown in Figure 9 and Table 1.

In Table 1, muhat is the mean value, sigmahat is the variance, muci is the 0.95 confidence interval of the mean value, sigmaci is the 0.95 confidence interval of the variance, and H is a Boolean variable. Here, $h = 0$ means that the null hypothesis is not rejected, which indicates that the hypothesis is reasonable. If sig is larger than 0.5, the null hypothesis cannot be rejected.

According to the inspection results in Figure 10 and Table 1, it can be seen that the flight acceleration error in the final

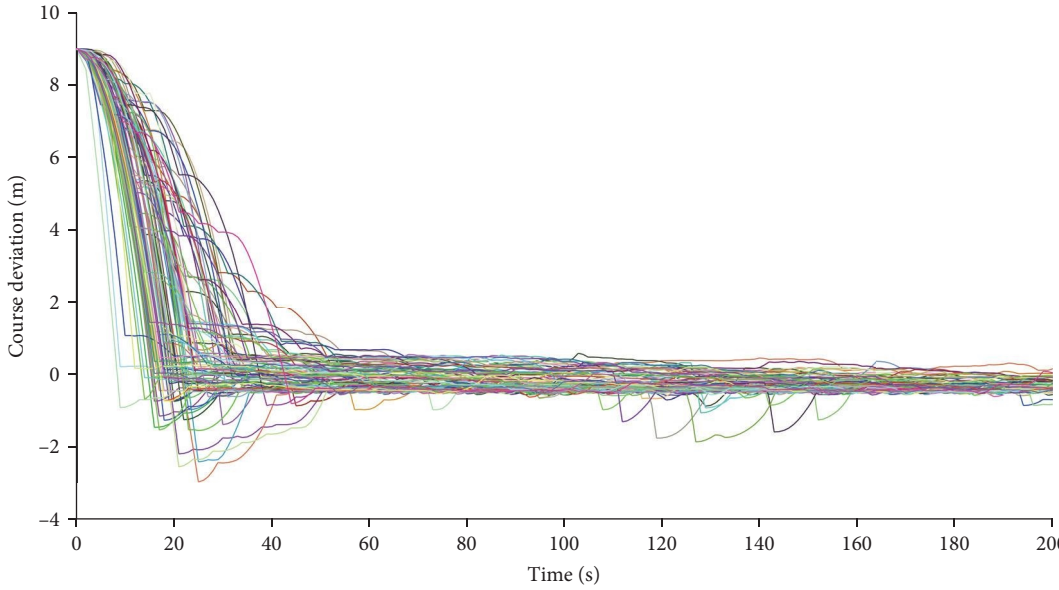

Figure 10: Simulation results of course deviation with 52% accuracy.

approach state obeys the normal distribution with a mean of −0.00281 and a standard deviation of 0.165198. Then, the probability density of acceleration error Δa_z is as follows:

$$f(\Delta a_z) = \frac{1}{\sqrt{0.330396\pi}} \exp\left(-\frac{(\Delta a_z + 0.00281)^2}{0.330396}\right). \quad (11)$$

A factor that cannot be ignored in the paired approach process is the movement of the wake. According to the characteristics of the diffusion and sinking of the wake, we establish the relationship model between the wake position of the trailing aircraft and the leading aircraft, where the formula is as follows:

$$\begin{cases} h(t) = h_{(b)} + V_{z(b)}t + \frac{1}{2}a_{z(b)}t^2 + \lambda_z + 2e(t) \\ S_0 = V_{x(b)}t_h + \frac{1}{2}a_{x(b)}{t_h}^2 \\ S_0 - V_{x(b)}t - \frac{1}{2}a_{x(b)}t^2 = V_{x0(p)}(\Delta t - t) + \frac{1}{2}a_{x0(p)}(\Delta t - t)^2, t < t_h \\ S_0 + \left(V_{x(p)} - V_{x(b)}\right)t + \frac{1}{2}\left(a_{x(p)} - a_{x(b)}\right)t^2 = \left(V_{x(p)} + a_{x(p)}t\right)\Delta t - \frac{1}{2}a_{x(p)}\Delta t^2, t > t_h \\ L_{z1}(t) = h_{(p)} + V_{z(p)}t + \frac{1}{2}a_{z(p)}t^2 + 2\lambda_z \\ L_{z2}(t) = h_{(p)} + V_{z(p)}t + \frac{1}{2}a_{z(p)}t^2 + \left(v_{(k)} + v_{(j)}\right)\Delta t + \frac{1}{2}\lambda_z, \left(v_{(k)} + v_{(j)}\right)\Delta t > \frac{3}{2}\lambda_z \\ L_{z2}(t) = h_{(p)} + V_{z(p)}t + \frac{1}{2}a_{z(p)}t^2, \left(v_{(k)} + v_{(j)}\right)\Delta t \le \frac{3}{2}\lambda_z, \end{cases} \quad (12)$$

where $h(t)$ is the height of the trailing aircraft, and $e(t)$ is the course deviation value of the aircraft at time t. We assume that there is no difference in the operating quality of the leading and trailing aircraft and take the leading aircraft as the reference, where the trailing aircraft runs with twice the deviation. $h_{(b)}$ and $h_{(p)}$ are the initial heights of the trailing and the leading aircraft in the final approach stage, $V_{z(b)}$ and $V_{z(p)}$ are the initial horizontal velocities of the trailing aircraft and the leading aircraft in the final approach stage, and $a_{z(b)}$ and $a_{z(p)}$ are the horizontal acceleration of the trailing aircraft and the trailing aircraft in the final approach stage. The velocity and acceleration are vector parameters, and λ_z is the average height of two aircraft's fuselage. Additionally, S_0 is the initial longitudinal distance between the two aircraft, $V_{x(b)}$ and $V_{x(p)}$ are the initial longitudinal velocities of the trailing aircraft and the leading aircraft in the final approach

Table 2: QAR data of the rudder pedal.

Course deviation (point)	Rudder pedal (°)	Rudder position (°)
0.665323	0.576236	0.317073
0.594758	0.576236	0.317073
0.524194	0.576236	0.253659
0.46371	0.576236	0.126829
0.413306	0.576236	0.190244
0.362903	0.576236	0.190244
0.322581	0.576236	0.126829
0.292339	0.576236	0.126829
0.252016	0.576236	0.190244
0.221774	0.576236	0.253659
0.181452	0.576236	0.190244
0.15121	0.576236	0.190244

stage, $a_{x(b)}$ and $a_{x(p)}$ are the longitudinal acceleration of the trailing aircraft and the leading aircraft, and t_h is the time taken by the trailing aircraft to fly over the initial distance S_0.

When the front aircraft does not reach the final approach point, its longitudinal acceleration is $a_{x0(p)}$, the longitudinal velocity at the final approach point of the trailing aircraft is $V_{x0(p)}$, and Δt is the dynamic time interval between two aircraft. $L_{z1}(t)$ is the height of the upper boundary of the horizontal overlapping area, $L_{z2}(t)$ is the height of the lower boundary of the horizontal overlapping area, $v_{(k)} < 0$ is the diffusion speed of the leading aircraft's wake, and $v_{(j)} < 0$ is the falling speed of the leading aircraft's wake.

In the paired approach, horizontal overlap is considered to occur when the trailing aircraft enters the wake of the leading aircraft from the horizontal direction or overlaps with the leading aircraft fuselage. The horizontal overlap probability is expressed by the following formula:

$$P_z = \frac{T_{L_{z1}(t) > h(t) > L_{z2}(t)}}{T}. \tag{13}$$

In the fuselage, $T_{L_{z1}(t) > h(t) > L_{z2}(t)}$ indicates the time when the trailing aircraft is in the horizontal overlapping area during the approach, and T is the total time during the final approach.

The horizontal overlapping frequency N_z is expressed as follows:

$$N_z = \frac{C_{L_{z1}(t) > h(t) > L_{z2}(t)}}{T}, \tag{14}$$

where $C_{L_{z1}(t) > h(t) > L_{z2}(t)}$ is the number of times that the trailing aircraft enters the horizontal overlapping area during the approach.

5. Simulation

Taking the QAR data of 30 aircraft landings at the same airport as the database, Table 2 shows the recorded data of the rudder pedal in the final approach stage. As shown in Table 2, pilots do not usually push the rudder for lateral control in the final approach stage (the reason for the change of rudder position is related to the crosswind and flight control system), so only lateral control is considered for lateral attitude adjustment in the approach.

The roll angle data from the database is employed as the action set, and the course deviation value is taken as the state set. The atmosphere density is 1.293 kg/m^3, the wing area is 109 m^2, the lift coefficient is 0.5, and the aircraft mass is 56,000 kg.

The above parameters are input into the model, the final approach time of the flight is set to 200 s, and the deviation value when entering the heading course is 9 m. According to the statistics, the correct rate of 30 flights is 52% minimum and 77% maximum. In the simulation, the correct rate of pilot operation is set to be 52%, 57%, 62%, 67%, 72%, and 77%, respectively, and each set of three correct rates is simulated 100 times. The simulation results are shown in Figures 10–15.

In this paper, first-line pilots are consulted about their operation experience of correcting the error of the course in the final approach stage. If there is a large left deviation when the aircraft enters the course, the pilots need to press the right lever to deflect the right aileron, so as to reduce the lift of the right wing and roll the aircraft to the right. Through the analysis of Formulas (3) and (5), it can be concluded that with the gradual increase of roll angle speed, the damping moment will also increase. When the moment reaches balance, the aircraft will roll at a certain angular speed, which will make the aircraft move sideways and gradually correct the course deviation. The whole correction process is also in line with the actual simulation results of the pilot operation model.

According to the simulation results, as the pilot's operating accuracy improves, the time it takes for the aircraft to adjust to the course is reduced. When the accuracy rate is 52%, it takes about 30 s on average, and when the accuracy rate is 77%, it takes about 15 s on average. However, no matter how much the accuracy rate improves, there will always be a situation in which the aircraft deviates from the course and then corrects back. This is due to the pilot's failure to properly adjust the slope of the aircraft in advance when approaching the course, which is related to the pilot's experience.

Although the simulation results with an operation accuracy of 52% and 77% can both stabilize the error at about 0 m after 60 s from the start of the final approach, a difference can still be found by comparing the two simulation results separately, as shown in Figure 16.

After 60 s, the heading deviation with an accuracy rate of 77% is relatively stable. However, the simulation results with an accuracy rate of 52% show that after the aircraft approaches the heading, it also experiences left–right deviations and the state is relatively unstable.

Figure 17 shows the historical operation data with a correct operation rate of about 52%, which indicate that the simulation results can show the actual operation process.

The pairing approach procedure stipulates that the altitude and glide angle of the trailing aircraft at the beginning of the procedure are larger than those of the leading aircraft [5], and the landing time of the two aircraft is similar, which makes

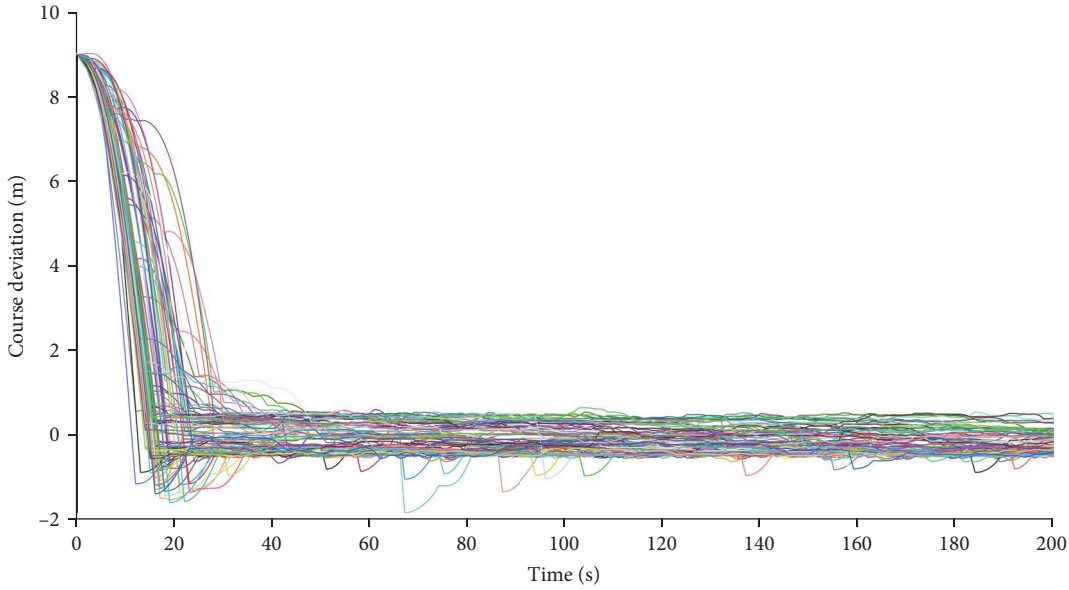

Figure 11: Simulation results of course deviation with 57% accuracy.

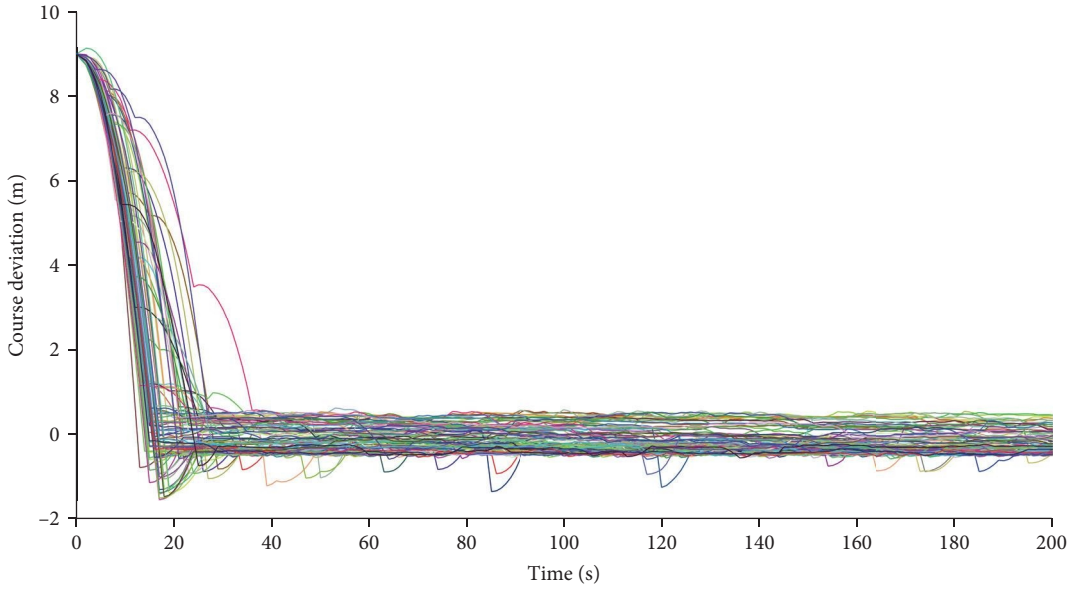

Figure 12: Simulation results of course deviation with 62% accuracy.

the velocity and acceleration of the trailing aircraft numerically larger than those of the leading one. According to the statistical results of the QAR data, the velocity of aircraft at the final approach point is usually 80 m/s. Here, the initial velocity of the front aircraft is 78 m/s, the initial longitudinal interval between the two aircraft is 2,000 m, and the time interval is 25 s. A crosswind wind speed of 1–2 m/s is considered a dangerous crosswind [25]. Here, it is taken as 2 m/s. The calculated operating parameters of the two aircraft are shown in Table 3.

Taking Shanghai Hongqiao Airport as an example, the interval between two runways is 365 m. According to statistics, the maximum error of an aircraft arriving at the final approach point is 20 m on the left and right. In the simulation, we assume that the error of the aircraft arriving at the fixed point obeys the following uniform distribution:

$$f(\varepsilon_0) = \begin{cases} \dfrac{1}{40}, & -20 \le \varepsilon_0 \le 20 \\ 0, & \text{other} \end{cases}. \tag{15}$$

Under the correct rate of 52%, the results of a million simulations are shown in Table 4, and overlapping time and number of overlaps are both zero.

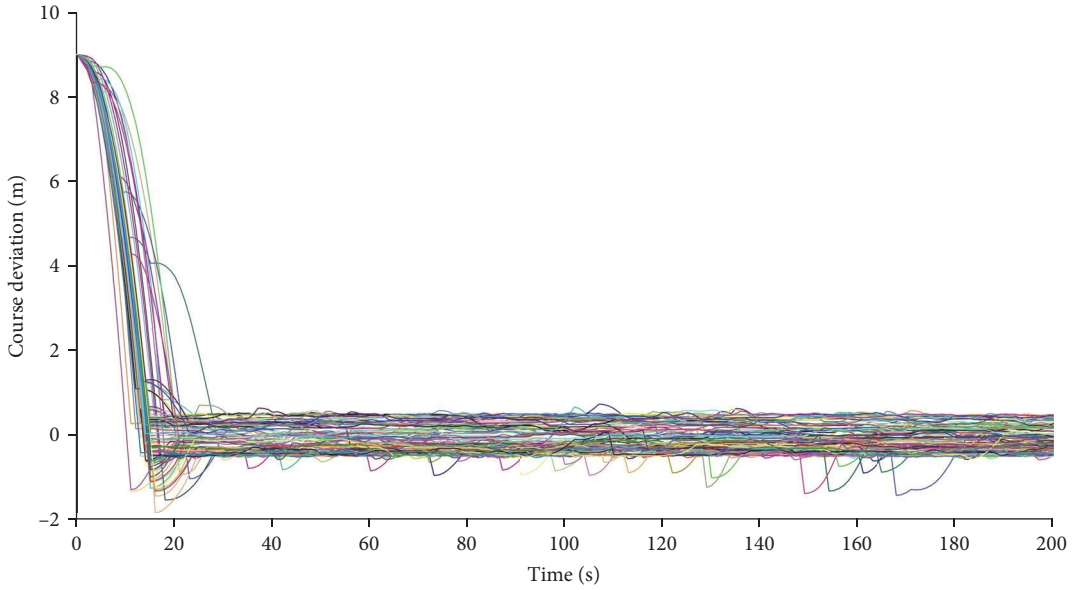

Figure 13: Simulation results of course deviation with 67% accuracy.

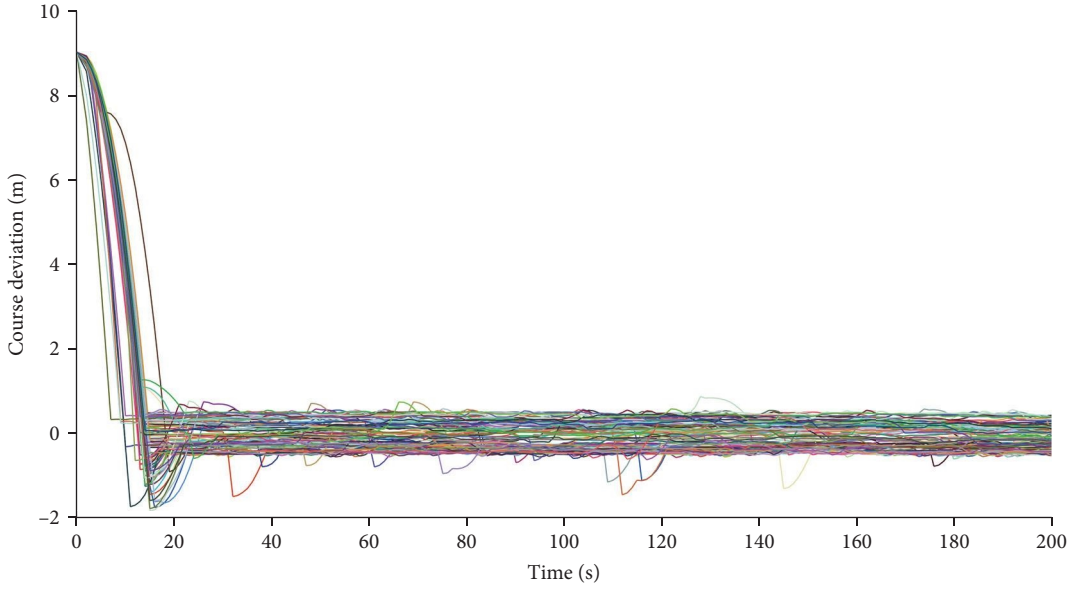

Figure 14: Simulation results of course deviation with 72% accuracy.

We then adjust the runway interval to 300 m, and situations of 52%–77% correct handling rate are simulated in turn. The simulation results are shown in Figure 18.

It can be seen from Figure 19 that the pilot's correct operation rate has little influence on the horizontal overlap probability and frequency, and the reason for this result can be explained through a simulation process.

Taking the simulation of an overlap as an example, the horizontal overlap situation is shown in Figure 18. It can be seen that the horizontal overlap between the wake of the leading aircraft and the trailing aircraft only occurs within 1–3 s before the beginning of pairing. According to the previous simulation results of course deviation, as time goes by, even if the operating accuracy is 52%, the trailing aircraft will be closer to the preset course, and the possibility of horizontal overlap with the wake of the leading aircraft will become increasingly smaller.

Therefore, in actual operation, in order to avoid horizontal overlap, the trailing aircraft should pay attention to the accuracy of entering a heading course at the beginning of the procedure.

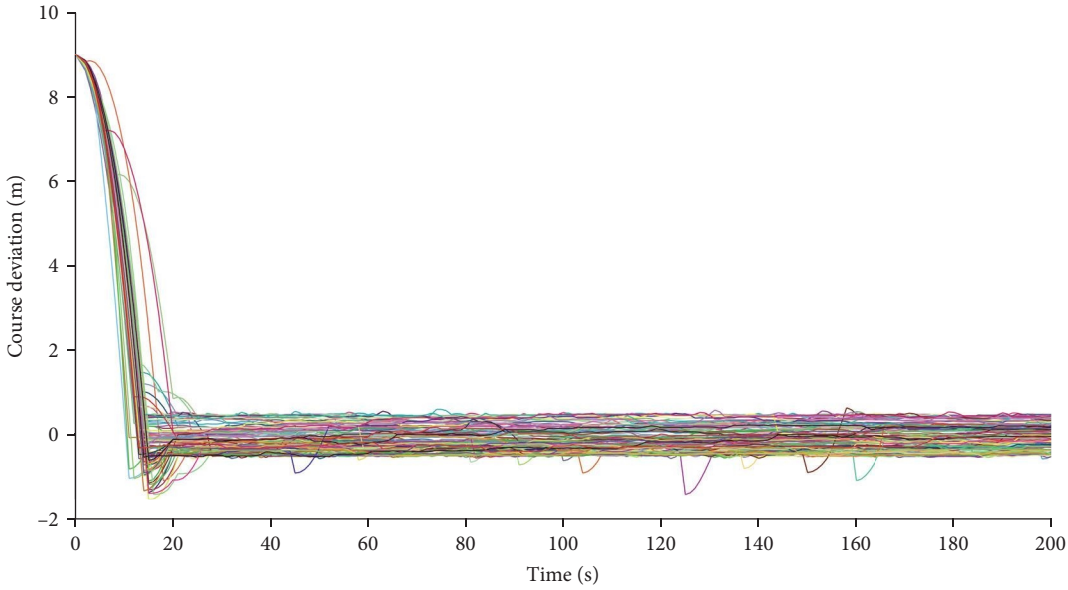

Figure 15: Simulation results of course deviation with 77% accuracy.

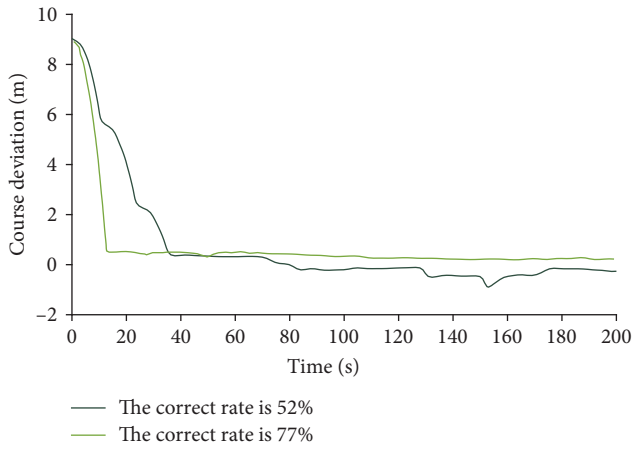

Figure 16: Comparison of course deviation with an accuracy of 52% and 77%.

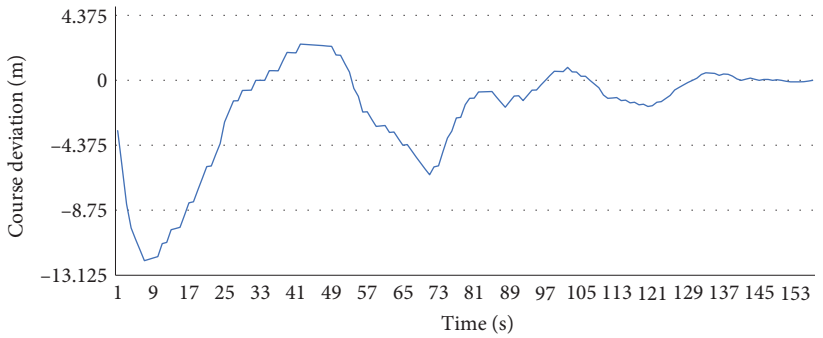

Figure 17: QAR operating data of 52% accuracy.

Table 3: Operating parameters.

Parameter	Leading aircraft	Trailing aircraft
Horizontal distance from runway entrance (m)	15,000	17,000
Glide slope (°)	2.5	3
Runway entrance speed (m/s)	72	
Longitudinal acceleration (m/s^2)	−0.03	−0.13
Longitudinal speed of final approach anchor point (m/s)	78	98
Final approach acceleration (m/s^2)	−0.16	—
Speed of the front aircraft at the last approach anchor point of the trailing aircraft (m/s)	82	—
Cross wind speed (m/s)	2	
Wake diffusion velocity (m/s)	1.5	

Table 4: Simulation results of Hongqiao Airport.

Horizontal overlap time (t)	Number of horizontal overlaps (times)	Horizontal overlap probability	Horizontal overlapping frequency (times·flight hours)
0	0	0	0

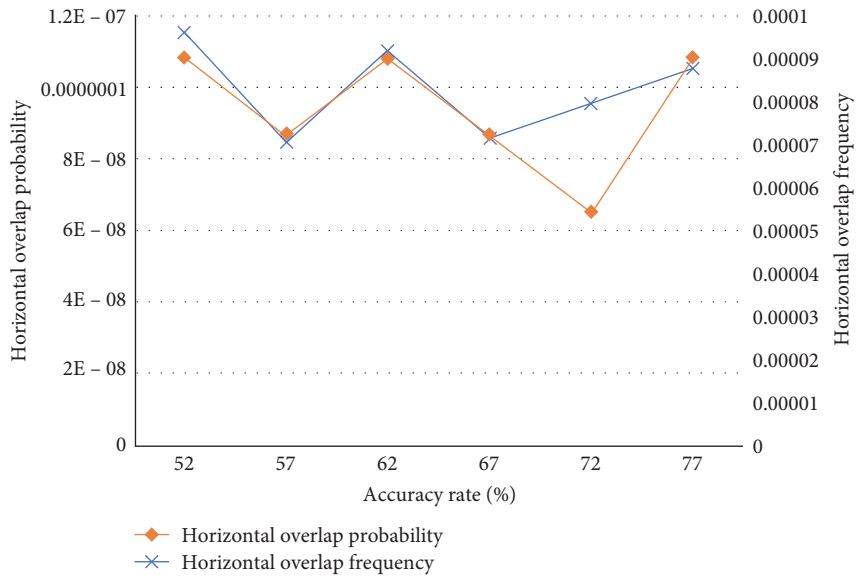

Figure 18: Simulation results of runway interval of 300 m.

In fact, if the trailing aircraft is on the side of the heading course away from the leading aircraft at the beginning of the procedure, the horizontal overlap can be better avoided.

6. Conclusion

(1) We establish a model for aircraft attitude adjustment based on the principle of flight mechanics and the characteristics of pilot operation. In this model, the operational parameters that have the highest correlation with the horizontal position error in the approach phase are considered. Subsequently, grounded in the standard statistical properties of these parameters, we employ the concept of a stochastic process to formulate a pilot operation model. These two models serve to elucidate the relationship between rudder control and the aircraft's lateral slip angle, as well as the interaction with the steering wheel and pitch angle.

(2) Considering the wake motion characteristics, we incorporate conditions for horizontal overlap into the establishment of a simulation model for paired approach scenarios. Through the execution of this simulation model, quantify both the horizontal overlap duration and the frequency of overlaps. Subsequently, the model was used to analyze the overlap probability and frequency under different pilot operation accuracy conditions.

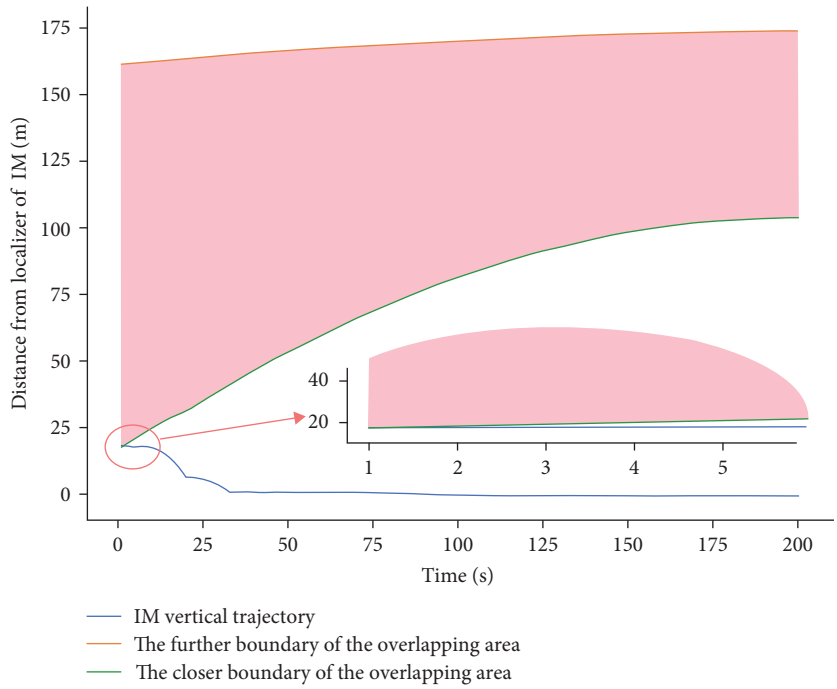

Figure 19: Schematic diagram of horizontal overlap.

(3) Combined with the above conclusion, therefore, the correct operation rate of the pilot has a relatively small impact on horizontal overlap; a higher pilot operational accuracy can shorten the adjustment time for horizontal deviation. Through collision risk analysis, it can be concluded that the horizontal overlap of the wake between two aircraft only occurs within 1–3 s before the pairing begins. Therefore, in actual operation, to avoid horizontal overlap, the rear aircraft should pay attention to the accuracy of adding a localizer at the beginning of the program.

Data Availability

The data used to support the findings of this study are available from the corresponding author upon request.

Conflicts of Interest

The authors declare that they have no conflicts of interest.

Acknowledgments

This work is supported by the National Natural Science Foundation of China (52272356) and the Fundamental Research Funds for the Central Universities (3122022101).

References

[1] M. C. Waller and C. H. Scanlon, *Proceedings of the NASA Workshop on Flight Deck Centered Parallel Runway Approaches in Instrument Meteorological Conditions*, NASA, Hampton, VA, 1996.

[2] W. Torres-Pomales, M. M. Madden, R. W. Butler, and R. B. Perry, *Analysis and Simulation of the Simplified Aircraft-Based Paired Approach Concept with the ALAS Alerting Algorithm in Conjunction with Echelon and Offset Strategies*, NASA, Hampton, Virginia, 2014.

[3] M. Geyer, M. Soares, S. Barnes, A. Hoff, and S. Mackey, *RNAV (GPS) Total System Error Models for Use in Wake Encounter Risk Analysis of Dependent Paired Approaches to Closely-Spaced Parallel Runways*, John A. Volpe National Transportation Systems Center (U.S.), 2013.

[4] S. Landry and A. R. Prichett, "The safe zone for paired closely spaced parallel approaches: implications for procedures and automation," in *19th DASC. 19th Digital Avionics Systems Conference. Proceedings (Cat. No.00CH37126)*, vol. 1, pp. 3E3/1–3E3/8, IEEE, Philadelphia, PA, USA, 2000.

[5] R. Teo, J. S. Jang, and C. Tomlin, "Flight demonstration of provably safe closely spaced parallel approaches," in *AIAA Guidance, Navigation, and Control Conference and Exhibit*, p. 6197, AIAA, San Francisco, California, 2005.

[6] M. M. Madden, "Kinematic modeling of separation compression for paired approaches to closely-spaced parallel runways," in *14th AIAA Aviation Technology, Integration, and Operations Conference*, p. 3150, NASA, Atlanta, GA, 2014.

[7] L. Fei, Z. Zhaoning, W. Zhiqiang, and L. Bilian, "The longitudinal collision risk assessment safety of closed parallel sheltered approaches," *China Safety Science Journal*, vol. 23, no. 8, pp. 108–113, 2013.

[8] L. Fei, Z. Nan, Y. Si, Z. Zhaoning, and L. Bilian, "Assessment on lateral collision risk of closed spaced parallel runways paired approach," *China Safety Science Journal*, vol. 26, no. 11, pp. 87–92, 2016.

[9] L. Zongping, Z. Zhaoning, and N. Xialei, "Collision risk safety assessment of paired approach based on velocity error and positioning error," *Aeronautical Computing Technique*, vol. 45, no. 6, pp. 36–40, 2015.

[10] G. Runping, W. Jun, and L. Fei, "Study on the closed spaced parallel runway paired approach procedure and collision risk," *Journal of Henan University of Science and Technology, Natural Science Edition*, vol. 40, no. 1, pp. 37–41, 2019.
[11] Z. Zhaoning and D. Xiaoxu, "Notice of retraction: model of paired departure from closely spaced parallel runways," in *2010 International Conference on Computer and Communication Technologies in Agriculture Engineering*, pp. 279–282, IEEE, Chengdu, China, June 2010.
[12] W. Lili, Z. Bo, and W. Fang, "Microscopic tracing model for the paired approach to the narrow-spaced parallel runways," *Journal of Safety and Environment*, vol. 17, no. 3, pp. 985–988, 2017.
[13] L. Fei, T. Jingjie, W. Jun, Z. Zhaoning, and Z. Zonglu, "Lateral collision risk of CSPRs paired approach under wake impact," *China Safety Science Journal*, vol. 30, no. 2, pp. 99–105, 2020.
[14] L. Fei, T. Jingjie, W. Jun, Z. Zhaoning, and Z. Zonglu, "Lateral collision dynamics of CSPRs paired approach under influence of wake vortex field," *China Safety Science Journal*, vol. 30, no. 4, pp. 21–27, 2020.
[15] L. Fei, L. Xinze, M. Mingjiang, and W. Zhiqiang, "Safety assessment of approximate segregated parallel operation on closely spaced parallel runways," *Chinese Journal of Aeronautics*, vol. 32, no. 2, pp. 463–476, 2019.
[16] L. Fei, C. Zichen, and C. Huiyu, "Lateral collision risk assessment of parallel routes in ocean area based on space-based ADS-B," *Transportation Research Part C: Emerging Technologies*, vol. 124, Article ID 102970, 2021.
[17] F. Lu, R. Sun, H. Chen, and Z. Chen, "Research on vertical overlap of the paired approach based on QAR," *IEEE Access*, vol. 10, pp. 94568–94582, 2022.
[18] P. G. Reich, "Analysis of long-range air traffic systems: separation standards—I," *Journal of Navigation*, vol. 19, no. 1, pp. 88–98, 1966.
[19] P. G. Reich, "Separation standards—II," *Journal of Navigation*, vol. 19, no. 2, pp. 169–186, 1966.
[20] P. G. Reich, "Analysis of long-range air traffic systems: separation standards—III," *Journal of Navigation*, vol. 19, no. 3, pp. 331–347, 1966.
[21] Z. Zhaoning, C. Zichen, and L. Fei, "Correlation analysis of QAR parameters for paired approach lateral position error," *China Safety Science Journal*, vol. 31, no. 8, pp. 47–52, 2021.
[22] L. R. Jenkinson, P. Sinpkin, and D. Rhodes, *Civil Jet Aircraft Design*, AIAA, 1999.
[23] K. Jianghong, W. Binliang, and L. Hongyan, *Aircraft Flight Dynamics*, Tsinghua University Publishing House, 2012.
[24] N. Guerreiro and K. Neitzke, "Simulated wake characteristics data for closely spaced parallel runway operations analysis," in *12th AIAA Aviation Technology, Integration, and Operations (ATIO) Conference and 14th AIAA/ISSMO Multidisciplinary Analysis and Optimization Conference*, AIAA, Indianapolis, Indiana, September 2012.
[25] M. L. Williams, L. C. Wood, and B. J. Nelson, "Safety study of closely spaced parallel operations utilizing paired approach," in *2019 IEEE/AIAA 38th Digital Avionics Systems Conference (DASC)*, pp. 1–10, IEEE, San Diego, CA, USA, September 2019.